

Analysis for efficiency potential of high-efficiency and next-generation solar cells

Masafumi Yamaguchi¹  | Kan-Hua Lee¹  | Kenji Araki¹  | Nobuaki Kojima¹ | Hiroyuki Yamada² | Yasuhiro Katsumata³

¹Toyota Technological Institute, Nagoya, Japan

²New Energy and Industrial Technology Development Organization, Kawasaki, Japan

³Japan Science and Technology Agency, Tokyo, Japan

Correspondence

Masafumi Yamaguchi, Toyota Technological Institute, 2-12-1 Hisakata, Tempaku, Nagoya 468-8511, Japan.

Email: masafumi@toyota-ti.ac.jp

Abstract

This paper overviews photovoltaic R&D projects in Japan. Recently, world-record and second highest efficiencies of various types of solar cells have been demonstrated under the New Energy and Industrial Technology Development Organization Project: 44.4% (under concentration) and 37.9% (under 1 sun) InGaP/GaAs/InGaAs inverted metamorphic 3-junction solar cells by Sharp, 26.7% single crystalline Si heterojunction back-contact solar cell by Kaneka, 22.3% copper indium gallium selenide solar cell by Solar Frontier, a-Si/ μ c-Si/ μ c-Si thin-film triple-junction solar cell with stabilized efficiency of 14.0% by AIST, 11.9% dye-sensitized solar cell by Sharp, and 11.2% organic solar cell by Toshiba. This paper also presents efficiency potential of high-efficiency and next-generation solar cells analyzed by considering external radiative efficiency, open-circuit voltage loss, and fill factor loss. Efficiency potential of crystalline Si, GaAs, III-V compound 3-junction and 5-junction, CIGSe, CdTe, CZTS(Se), multiquantum well, and quantum dot and perovskite solar cells is shown to be 28.5%, 29.7%, 40%, 43%, 26.5%, 26.5%, 20%, 25.8%, and 24.9% under 1 sun, respectively.

KEYWORDS

CdTe, CIGS, crystalline Si, CZTS(Se), external radiative efficiency, III-V multijunction, MQW and QD, perovskite

1 | INTRODUCTION

The solar electricity including solar photovoltaics (PVs) is expected to contribute as the main energy with a share of about 20% and 70% in 2050 and 2100, respectively, in total energy of the world, according to the recommendation (World Energy Vision 2100) by the German Advisory Council on Global Change.¹ The Fukushima nuclear power plant accident that occurred in March 2011 has given us very important messages such as unclearness for safety and cost effectiveness of nuclear energy and importance of clean renewable energies including PV instead of nuclear energy. These suggest importance of further development of science and technology of PV and international collaboration and cooperation for PV. Even in Japan, more than 40 years of national PV R&D programs were conducted since 1974, and cumulative PV system installation in Japan reached more than 40 GW in 2016 due to feed-in-tariff, subsidy, and R&D programs. The cumulative

PV system installation by 2030 in Japan is 100 GW under the New Energy and Industrial Technology Development Organization (NEDO)'s PV2030 Roadmap [2]. For this end, further development of science, technology, and deployment of PVs is necessary.

This paper presents brief overviews of PV R&D projects in Japan as the project leader of the project "High Performance Photovoltaic System Technology Development for the Future" under the NEDO and the research supervisor of the research area "Creative Clean Energy Generation by using Solar Energy" under the JST.

To discuss about future direction of PV R&D, efficiency potential of various solar cells should be clarified. This paper also discusses about efficiency potential of high-efficiency solar cells such as crystalline Si, GaAs, III-V compound multijunction, CIGSe ($\text{CuInGa}(\text{S,Se})_2$) and CdTe solar cells, and next-generation solar cells such as CIGS (CuInGaS_2), CZTS(Se) ($\text{Cu}_2\text{ZnSn}(\text{S,Se})_4$), MQW (multiquantum well), QD (quantum dot), perovskite, and ferroelectric solar cells.

2 | BRIEF OVERVIEW OF PHOTOVOLTAIC RESEARCH AND DEVELOPMENT PROJECTS IN JAPAN

This paper presents brief overviews of PV R&D projects in Japan as the project leader of the project "High Performance Photovoltaic System Technology Development for the Future" under the NEDO and the research supervisor of the research area "Creative Clean Energy Generation by using Solar Energy" under the JST. Recently, world-record and second highest efficiencies of various types of solar cells have been demonstrated under the NEDO Project: 44.4% (under concentration) and 37.9% (under 1 sun) InGaP/GaAs/InGaAs inverted metamorphic 3-junction solar cells by Sharp, 26.7% single crystalline Si heterojunction back-contact (HBC) solar cell by Kaneka, 22.3% CIGS solar cell by Solar Frontier, a-Si/ μ c-Si/ μ c-Si thin-film triple-junction solar cell with stabilized efficiency of 14.0% by AIST, 11.9% dye-sensitized solar cell by Sharp, and 11.2% organic solar cell by Toshiba.

Table 1 shows present status of various types of solar cells as a measure of current 1-sun conversion efficiency achieved and Japanese contribution. Due to national PV R&D projects in Japan, a Japanese group has contributed to achievement of world-record and second highest efficiencies of various types of solar cells.

Various solar cells and materials have great potential as major solar cells and materials including single crystalline Si, III-V multijunction cells, CIGSe, and CdTe cells are expected to have great potential of terrestrial application because of high efficiency, light weight, and low cost potential. However, there are some problems to be solved for further development of high-efficiency solar cells. Because point defects even in crystalline Si, dislocations, and interface recombination in CIGSe and CdTe solar cell materials affect solar cell properties, understanding and controlling those defects are very important for realizing higher efficiency. Most recently, 26.7% efficiency has also been demonstrated with HBC Si solar cell by Kaneka.¹ However, even crystalline Si solar cells have nonradiative loss and further improvements in efficiency are thought to be possible by improving minority-carrier lifetime and reducing recombination losses.

TABLE 1 Present status of various types of solar cells as a measure of current 1-sun conversion efficiency achieved at laboratories and Japanese contribution

	Materials	Efficiency (%)
I (Si)	Single-Si	26.7 (Kaneka)
	Poly-Si	21.3
II (Thin film)	a-Si/ μ c-Si 3-junction	14.0 (AIST)
	CuInGaSe ₂	22.6
	CdTe	22.1
III (III-V)	GaAs	28.8
	InP	22.1
	3-junction	37.9 (Sharp)
	5-junction	46.0
Future generation	Perovskite	22.1
	Dye-sensitized	11.9 (Sharp)
	Organic	11.2 (Toshiba)

3 | ANALYTICAL PROCEDURE FOR ESTIMATING EFFICIENCY POTENTIAL OF SOLAR CELLS

Radiative recombination lifetime τ_{rad} is expressed by

$$\tau_{\text{rad}} = 1/BN \quad (1)$$

where N is carrier concentration and B is radiative recombination probability. For Si and GaAs, B values are $2 \times 10^{-15} \text{ cm}^3/\text{s}$ and $2 \times 10^{-10} \text{ cm}^3/\text{s}$,² respectively. Therefore, optimization of carrier concentration in solar cell layers is necessary by considering minority-carrier lifetime and series resistance. In addition, photon recycling is also important to reduce the impact of radiative recombination and to give lower effective B . Effective lifetime τ_{eff} is expressed by

$$1/\tau_{\text{eff}} = 1/\tau_{\text{rad}} + 1/\tau_{\text{nonrad}} \quad (2)$$

where τ_{nonrad} is nonradiative recombination lifetime and given by

$$1/\tau_{\text{nonrad}} = \sigma v N_r \quad (3)$$

where σ is capture cross section of minority carriers by nonradiative recombination centers, v is minority-carrier thermal velocity, and N_r is density of nonradiative recombination centers such as bulk defects, surface states, interface states, and so forth. Therefore, improvements in crystalline quality and reduction in densities of defects such as point defects, dislocations, grain boundaries, interface states, and impurities that act as nonradiative recombination centers are very important.

To realize higher efficiency of various solar cells, improvements in short-circuit density (J_{sc}), open-circuit voltage (V_{oc}), and fill factor (FF) are substantially necessary.

The V_{oc} is given by

$$V_{\text{oc}} = \frac{kT}{q} \ln \left(\frac{J_L}{J_0} + 1 \right) \quad (4)$$

where k is Boltzmann constant, T is absolute temperature, q is electronic charge, J_L is photon-generated current density, and J_0 is saturation current density. To increase V_{oc} , decrease in saturation current density J_0 is essential.

One of the problems to attain the higher efficiency solar cells is the higher minority-carrier lifetime in various materials. Figure 1 shows

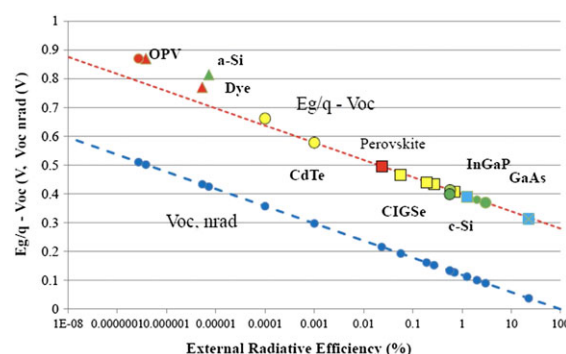


FIGURE 1 Open-circuit voltage (V_{oc}) drop compared with bandgap energy ($E_g/q - V_{\text{oc}}$) and nonradiative V_{oc} ($V_{\text{oc}}, \text{nrad}$) in various solar cells as a function of external radiative efficiency (ERE) [Colour figure can be viewed at wileyonlinelibrary.com]

V_{oc} drop compared with bandgap energy ($E_g/q - V_{oc}$) and nonradiative voltage loss ($V_{oc,rad}$) in various solar cells as a function of external radiative efficiency (ERE). Open-circuit voltage is expressed by³⁻⁵

$$V_{oc} = V_{oc,rad} + \frac{kT}{q} \ln(ERE) \quad (5)$$

where the second term shows nonradiative voltage loss and $V_{oc,rad}$ is radiative V_{oc} and is given by³⁻⁵

$$V_{oc,rad} = \frac{kT}{q} \ln \left(\frac{J_L(V_{oc,rad})}{J_{0,rad}} + 1 \right) \quad (6)$$

where $J_L(V_{oc,rad})$ is photocurrent at open circuit in the case of only radiative recombination, $J_{0,rad}$ is saturation current density in the case of only radiative recombination, and $V_{oc,rad}$ is nonradiative voltage loss and shows the second term in Equation 5.

Table 2 shows ERE, voltage losses, and other parameters for various materials and solar cells.^{1,4-17} 0.23 V for CZTS and CZTSSe cells, 0.28 V for MQW and QD cells, and 0.25 V for Perovskite cells were used as the $\Delta V_{oc,rad} = E_g/q - V_{oc,rad}$ value^{5,8} in this study. V_{oc} shows experimental value reported in Yoshikawa et al, Green, and Okada et al.^{1,4-17} Voltage losses and other parameters in the reference were estimated from Equation 5 by assuming 0.26 V for Si, 0.28 V for GaAs, 0.25 V for Perovskite, and 0.23 V for other materials⁵ as $\Delta V_{oc,rad} = E_g/q - V_{oc,rad}$. E_g in the table was estimated from the external

quantum efficiency spectrum in the references. The E_g value in the table was estimated by considering band tail in the external quantum efficiency spectrum in the references.

Because ERE for crystalline Si cells reported is 0.57%,⁴ even crystalline Si solar cells have nonradiative loss and further improvements in efficiency are thought to be possible by improving minority-carrier lifetime and reducing recombination losses.

Fill factor is dependent upon V_{oc} , and ideal fill factor FF_0 used in the calculation is empirically expressed by¹⁸

$$FF_0 = \frac{v_{oc} - \ln(v_{oc} + 0.72)}{v_{oc} + 1} \quad (7)$$

where v_{oc} is normalized V_{oc} and is given by

$$v_{oc} = V_{oc}/(nkT/q) \quad (8)$$

The FF is decreased as increase in series resistance R_s and decrease in shunt resistance R_{sh} of solar cell and expressed by¹⁸

$$FF \approx FF_0(1-r_s)(1-1/r_{sh}) \approx FF_0(1-r_s-1/r_{sh}) \quad (9)$$

where r_s and r_{sh} are normalized series resistance and normalized shunt resistance, respectively, and are given by

$$r_s = R_s/R_{CH} \quad (10)$$

TABLE 2 External radiative efficiency (ERE), voltage losses, and other parameters for various materials and solar cells

Solar Cell	E_g (eV)	V_{oc} (V)	$V_{oc,rad}$ (V)	$\Delta V_{oc,rad}$ (V)	$V_{oc,nrad}$ (V)	ERE (%)	Reference No
c-Si	1.12	0.68	0.86	0.26	0.18	0.1	7
	1.12	0.706	0.86*	0.26*	0.154*	0.21***	6
	1.12	0.721	0.86*	0.26*	0.139*	0.46***	6
	1.12	0.740	0.86*	0.26*	0.12*	0.98***	3
GaAs	1.42	1.11	1.146	0.279	0.036	22.5	6,7
	1.42	1.03	1.146	0.28*	0.116*	1.26	6
InGaP	1.805	1.452	1.518	0.287	0.066	8.29	10
	1.810	1.458	1.521	0.287	0.063	8.71	10
CIGSe	1.18	0.74	0.95	0.23	0.21	0.03***	6,7
	1.08	0.711	0.85*	0.23*	0.139*	0.46***	11
	1.13	0.741	0.90*	0.23*	0.159*	0.21***	12
	1.16	0.776	0.93*	0.23*	0.154*	0.26***	13
CdTe	1.45**	0.838	1.22*	0.23*	0.357*	1×10^{-4}	6,9
a-Si	1.72(1.6)**	0.886	1.49 (1.32)*	0.23*	0.604 (0.484)*	5.3×10^{-6}	6,8
Dye	1.51(1.32)**	0.719	1.28 (1.12)*	0.23*	0.561 (0.401)*	7.2×10^{-6}	6,9
Organic	1.72(1.55)**	0.816	1.49 (1.32)*	0.23*	0.674 (0.504)*	2.7×10^{-7}	6,9
	1.61(1.46)*	0.759	1.38 (1.23)*	0.23*	0.621 (0.470)*	3.8×10^{-7}	6,8
CIGS	1.55	0.954	1.32*	0.23*	0.366*	7.2×10^{-5} ***	14
CZTS	1.45	0.71	1.22*	0.23*	0.51*	2.8×10^{-7} ***	15
CZTSSe	1.13	0.5134	0.90*	0.23*	0.387*	3.2×10^{-5} ***	16
	1.07	0.502	0.84*	0.23*	0.338*	2.2×10^{-4} ***	17
MQW	1.42	0.94	1.146*	0.28*	0.206*	0.035***	18
QD	1.42	0.90	1.146*	0.28*	0.246*	7.4×10^{-3} ***	19
Perovskite	1.61	1.08	1.33	0.25	0.28	2×10^{-3} ***	7
	1.55	1.105	1.30*	0.25*	0.195*	0.053***	12

V_{oc} shows experimental value reported in references Yoshikawa et al, Green, and Okada et al.^{1,4-17}

*Voltage losses and other parameters estimated from Equation 5 by assuming 0.26 V for Si, 0.28 V for GaAs, 0.25 V for perovskite, and 0.23 V for other materials⁵ as $\Delta V_{oc,rad} = E_g/q - V_{oc,rad}$.

** E_g estimated from the external quantum efficiency (EQE) spectrum. The E_g value was estimated by considering band tail in the EQE spectrum.

***ERE estimated from Equation 5. Unmarked voltage losses, E_g , and ERE values show values from Green, Yao et al, and Geisz et al.^{4,5,8}

$$r_{sh} = R_{sh}/R_{CH} \quad (11)$$

The characteristic resistance R_{CH} is expressed by¹⁸

$$R_{CH} = \frac{V_{oc}}{I_{sc}} \quad (12)$$

In the calculation, highest values obtained were used as J_{sc} . V_{oc} and FF were calculated by Equations 5 to 9 and conversion efficiency potential of various solar cells were calculated as a function of ERE.

4 | ANALYSIS FOR EFFICIENCY POTENTIAL OF HIGH-EFFICIENCY SOLAR CELLS

4.1 | Efficiency potential of crystalline Si solar cells

Figure 2 shows V_{oc} drop compared with bandgap energy ($E_g/q - V_{oc}$) and nonradiative voltage loss ($V_{oc, nr}$) in Si solar cells as a function of ERE. In Si, 0.26 V was used as the $\Delta V_{oc, nr}$ value.⁵ In the figure, V_{oc} values for HIT (heterojunction with intrinsic thin layer) cell,¹⁹ HBC cells,^{1,20} PERL (passivated emitter and rear locally diffused) cell,^{4,5,21} and multicrystalline Si cell²² and ERE values estimated by using Equation 5 are plotted except for PERL cell.⁴ The HIT cells have better ERE compared with HBC and PERL cells. Multicrystalline cells have lower ERE values due to lower minority-carrier lifetime. As shown in Figure 2, crystalline Si solar cells have nonradiative loss, and further improvements in efficiency are thought to be possible by improving minority-carrier lifetime and reducing recombination losses.

Figure 3 shows calculated efficiency of crystalline Si solar cells as a function of ERE and efficiency values for PERL cell,⁴ HIT cell,¹⁹ and HBC cell^{1,20} as a function of ERE. In the figure, ERE values estimated by using Equation 5 are plotted except for PERL cell.⁴ Although the PERL cell shows the highest J_{sc} , improvement in V_{oc} is a problem to be solved. On the other hand, regarding the HIT cell shows the highest V_{oc} , improvement in J_{sc} is a problem to be solved. The HBC cells have potential of higher V_{oc} and J_{sc} . In summary, efficiencies over 28% such as 28.0%, 28.5%, and 28.8% will be realized with $r_s + 1/r_{sh}$ of 0.05 by improvements in ERE into 10%, 20%, and 30%, respectively, from around 1% as shown in Figure 3.

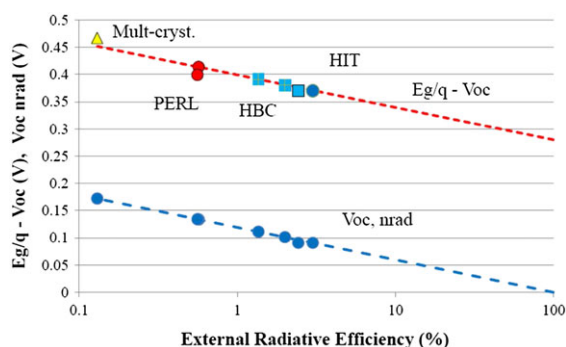


FIGURE 2 Open-circuit voltage (V_{oc}) drop compared with bandgap energy ($E_g/q - V_{oc}$) and nonradiative V_{oc} ($V_{oc, nr}$) in Si solar cells as a function of external radiative efficiency (ERE) [Colour figure can be viewed at [wileyonlinelibrary.com](#)]

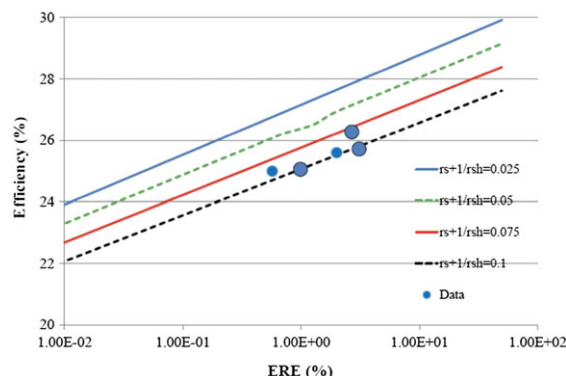


FIGURE 3 Calculated efficiency of crystalline Si solar cells as a function of external radiative efficiency (ERE) and $r_s + 1/r_{sh}$ in comparison with efficiencies of PERL, HIT, and HBC cells [Colour figure can be viewed at [wileyonlinelibrary.com](#)]

4.2 | Efficiency potential of various high-efficiency solar cells

Efficiency potential of high-efficiency solar cells such as crystalline Si, GaAs, GaAs/Si, CIGSe, and CdTe solar cells has been discussed based on ERE, V_{oc} loss, and FF loss. Detail results will be presented elsewhere.

Figure 4 shows summary for potential efficiencies of various high-efficiency solar cells.

In summary, crystalline Si solar cells have potential efficiency of 28.8% with normalized series resistance and shunt resistance $r_s + 1/r_{sh}$ of 0.05 by improvements in ERE from around 1% to 30%. GaAs have potential efficiency of 30.0% with $r_s + 1/r_{sh}$ of 0.025 by improvements in ERE from 22.5% to 40%. III-V 3-junction and 5-junction cells have potential efficiencies of 40% and 43% with $r_s + 1/r_{sh}$ of 0.05 by improvements in ERE from 0.05% to 1% and from 0.005% to 1%, respectively. CuInGa(S,Se)₂ and CdTe cells have potential efficiencies of 26.5% and 26.4% with $r_s + 1/r_{sh}$ of 0.05 by improvements in ERE from around 0.5% to 10% and from around 0.1% to 5%, respectively. Perovskite cells have potential efficiency of 24.9% by improvements in ERE from around 0.1% to 5%.

For this end, further improvements in minority-carrier lifetime based on understanding defect behavior in addition to improvements in front surface, rear surface, and interface passivation and decrease

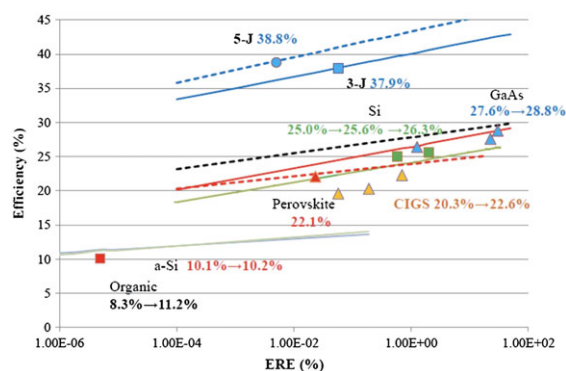


FIGURE 4 Calculated efficiencies of various solar cells as a function of external radiative efficiency (ERE) in comparison with efficiencies obtained [Colour figure can be viewed at [wileyonlinelibrary.com](#)]

in series resistance and increase in shunt resistance are suggested to realize higher efficiency solar cells.

5 | ANALYSIS FOR EFFICIENCY POTENTIAL OF NEXT-GENERATION SOLAR CELLS

5.1 | Efficiency potential of CZTS, CZTSSe, and CIGS solar cells

The CZTS ($\text{Cu}_2\text{ZnSnS}_4$) and CZTSSe solar cells²³ have drawn worldwide attention due to earth-abundant composition and high-efficiency potential. On the other hand, the CIGS solar cells have higher efficiency potential compared with conventional $\text{Cu}(\text{In,Ga})\text{Se}_2$ solar cells because CIGS has optimum band gap energy of about 1.5 eV.¹²

Figure 5 shows V_{oc} drop compared with bandgap energy ($E_g/q - V_{oc}$) and nonradiative voltage loss (V_{oc} , nrad) in CIGSe (CuInGaSe_2), CIGS, CdTe, CZTS, and CZTSSe solar cells^{4,6,7,9,10,14,15,24,25} as a function of ERE. In the figure, ERE values estimated by using Equation 5 are plotted except for CIGSe cells reported by ZSW and NREL^{4,6,7} and CdTe cell reported by ASP.^{4,6,7} Approximately 0.23 V was used as the ΔV_{oc} , rad value⁵ in CIGSe, CIGS, CdTe, CZTS, and CZTSSe.

As shown in Figure 5, CIGSe and CdTe solar cells have nonradiative loss, and further improvements in efficiency are thought to be possible by improving minority-carrier lifetime and reducing recombination losses. In addition, CZTS, CZTSSe, and CIGS solar cells have much larger nonradiative recombination loss compared with those in CIGSe and CdTe cells.

Figure 6 shows calculated efficiency of CZTS, CZTSSe, and CIGSe solar cells as a function of ERE⁵ and efficiency values for CZTS and CZTSSe cells reported by Solar Frontier^{24,25} and IBM^{14,22} and CIGSe cells reported by Solar Frontier,⁹ ZSW,^{4,6,7} and NREL.^{4,6,7} At present, although high efficiency of 22.3% and 22.6% has been attained with the CIGSe cells,^{9,22} CZTSSe cell has shown much lower efficiency of 12.6%,^{10,18} and thus, there are some problems to be solved.

In summary, in the CZTS and CZTSSe solar cells, efficiencies over 20% from present 12.6% efficiency¹⁴ will be realized with $r_s + 1/r_{sh}$ of 0.2 by improvements in ERE into more than 1% from about 0.001% as

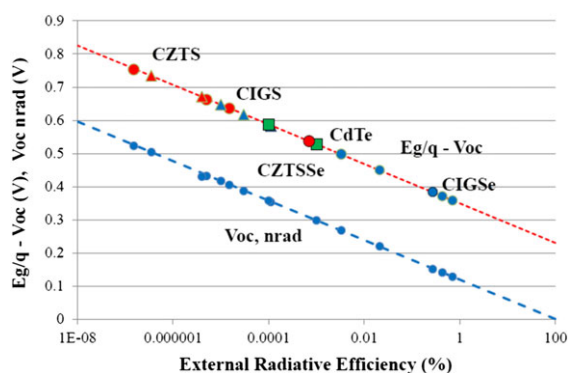


FIGURE 5 Open-circuit voltage (V_{oc}) drop compared with bandgap energy ($E_g/q - V_{oc}$) and nonradiative V_{oc} (V_{oc} , nrad) in CIGSe, CIGS, CdTe, CZTS, and CZTSSe solar cells as a function of external radiative efficiency (ERE) [Colour figure can be viewed at wileyonlinelibrary.com]

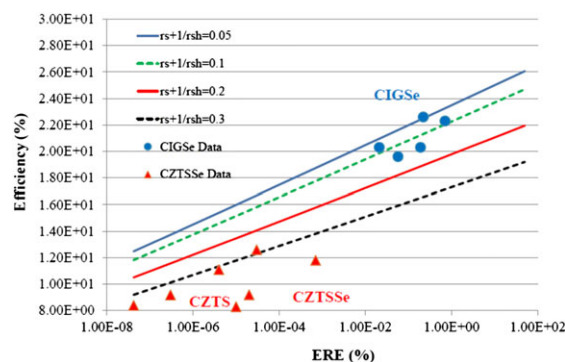


FIGURE 6 Calculated efficiency of CZTS, CZTSSe, and CIGSe solar cells as a function of external radiative efficiency (ERE) and $r_s + 1/r_{sh}$ in comparison with efficiencies of CZTS, CZTSSe, and CIGSe solar cells reported [Colour figure can be viewed at wileyonlinelibrary.com]

shown in Figure 6. To improve ERE in CZTS and CZTSSe cells, improvements in nonradiative recombination losses in active layers and interfaces are based on understanding defects and interface in those cells. Although efficiency potential of CIGS solar cells is not shown in the figure, ERE values of CIGS solar cells are also lower (about 0.001%) compared with CIGSe solar cells. Therefore, in the CIGS solar cells, efficiencies more than 22% from present 16.9% efficiency¹² will also be realized by improvements in ERE into more than 1% from about 0.001%.

5.2 | Efficiency potential of MQW and QD solar cells

The MQW solar cells²⁶ and QD solar cells²⁷ have also drawn worldwide attention due to its high-efficiency potential. However, interface recombination needs to be solved for realizing high-efficiency MQW and QD cells. Figure 7 shows V_{oc} drop compared with bandgap energy ($E_g/q - V_{oc}$) and nonradiative voltage loss (V_{oc} , nrad) in GaAs cells,^{4,22,28} MQW cells,¹⁶ and QD cells^{17,29-31} as a function of ERE. In the figure, ERE values estimated by using Equation 5 are plotted except for GaAs cells reported by Alta Devices.^{4,22,28}

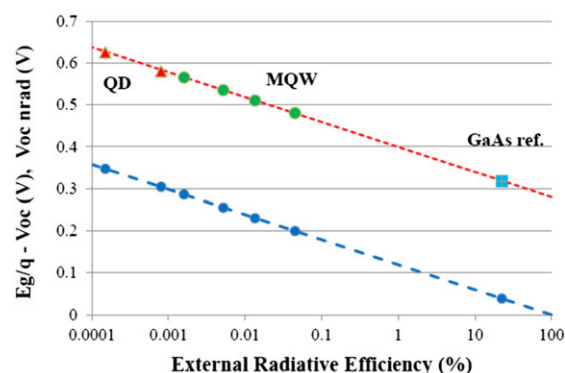


FIGURE 7 Open-circuit voltage (V_{oc}) drop compared with bandgap energy ($E_g/q - V_{oc}$) and nonradiative V_{oc} (V_{oc} , nrad) in GaAs, MQW, and QD solar cells as a function of external radiative efficiency (ERE) [Colour figure can be viewed at wileyonlinelibrary.com]

Average value of 0.28 V for GaAs and InGaP^{4,8} was also used as the $\Delta V_{oc,rad}$ value for MQW and QD.

As shown in Figure 7, higher ERE values of 22.5%⁴ and 8.71%⁸ for GaAs and InGaP solar cells, respectively, have been obtained due to high-quality thin-layer, reducing front and rear surface and interface recombination, and optical management.^{8,28} On the other hand, MQW and QD solar cells have much larger voltage drop due to lower ERE values of less than 0.1%. Therefore, reduction in nonradiative recombination loss such as interface recombination is necessary.

Lattice mismatching also degrades solar cell properties by increase in interface recombination velocity due to misfit dislocations and threading dislocations generation. Figure 8 shows interface recombination velocity S_i as a function of lattice mismatch ($\Delta a/a_0$) for InGaP/GaAs heteroepitaxial interface.³² Lattice mismatch ($\Delta a/a_0$) dependence of interface recombination velocity (S_i) is semiempirically expressed by³³

$$S_i[\text{cm/s}] = 1.5 \times 10^8 \Delta a/a_0 \quad (13)$$

Reduction in interface recombination by decreasing lattice mismatch is necessary to realize high-efficiency MQW and QD solar cells.

Figure 9 shows calculated efficiency of MQW and QD solar cells as a function of ERE and efficiency values for GaAs solar cells by Alta Devices^{4,22,28} and FhG-ISE^{4,6,7} and MQW and QD cells reported by Ioffe Inst,²⁹ Rochester Inst,³¹ and Univ Tokyo^{16,17,30} as a function of ERE.⁴ Although the GaAs solar cells have realized highest ERE of 22.5%,⁴ MQW and QD solar cells have much lower ERE of less than 0.1%. Further improvement in efficiency is also thought to be possible by improving minority-carrier lifetime and reducing nonradiative recombination losses due to increasing ERE and decreasing $r_s + r_{sh}$. In summary, efficiencies over 24% such as 24.8% and 25.8% will be realized with $r_s + 1/r_{sh}$ of 0.1 by improvements in ERE into 1% and 10%, respectively, from 0.1% as shown in Figure 9. However, because interface recombination is substantial problem in lattice mismatched systems such as MQW and QD solar cells, it is difficult to realize higher efficiency than conventional GaAs solar cells by using the MQW and QD solar cells.

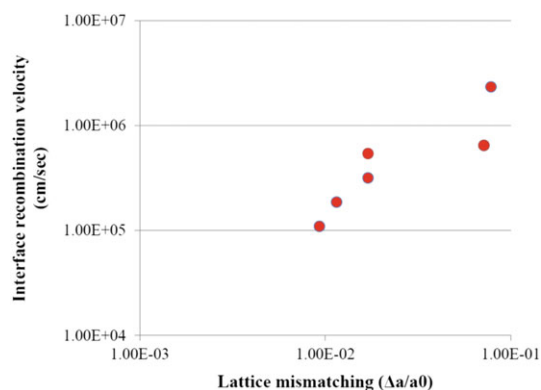


FIGURE 8 Interface recombination velocity S_i as a function of lattice mismatch ($\Delta a/a_0$) for InGaP/GaAs heteroepitaxial interface [Colour figure can be viewed at [wileyonlinelibrary.com](#)]

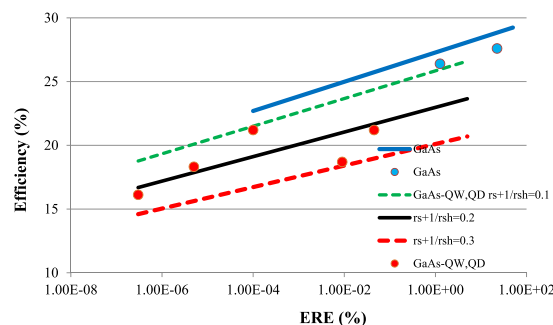


FIGURE 9 Calculated efficiency of MQW and QD solar cells as a function of external radiative efficiency (ERE) and $r_s + 1/r_{sh}$ in comparison with efficiencies of GaAs solar cells reported by Alta Devices and FhG-ISE and MQW and QD cells reported by Imperial College, Ioffe Inst Rochester Inst, and Univ Tokyo [Colour figure can be viewed at [wileyonlinelibrary.com](#)]

5.3 | Efficiency potential of perovskite solar cells

The perovskite solar cells³⁴ have also drawn worldwide attention due to low-cost and high-efficiency potential. However, device physics of the perovskite cells is still unknown.

Figure 10 shows V_{oc} drop compared with bandgap energy ($E_g/q - V_{oc}$) and nonradiative voltage loss ($V_{oc, nrad}$) in perovskite solar cells^{22,35} as a function of ERE. In the figure, ERE values estimated by using Equation 5 are plotted. In perovskite solar cells, 0.25 V was used as the $\Delta V_{oc,rad}$ value.⁵

As shown in Figure 10, perovskite solar cells have lower ERE of around 0.02% compared with 22.5% for GaAs⁴ and 8.71% for InGaP,⁸ and still nonradiative loss and further improvements in efficiency are thought to be possible by improving minority-carrier lifetime and reducing recombination losses.

Figure 11 shows calculated efficiency of perovskite solar cells as a function of ERE⁴ and efficiency values for perovskite solar cells reported by KRICT^{22,35} and EPFL.³⁶ In summary, in the perovskite solar cells, efficiencies over 24% such as 24.0% and 24.9% from present 22.1% efficiency³⁵ will be realized with $r_s + 1/r_{sh}$ of 0.1 by improvements in ERE into 1% and 10%, respectively, from around 0.02% as shown in Figure 11. In addition, solving reliability of the perovskite solar cells and replacing Pb and I with harmless materials are necessary.

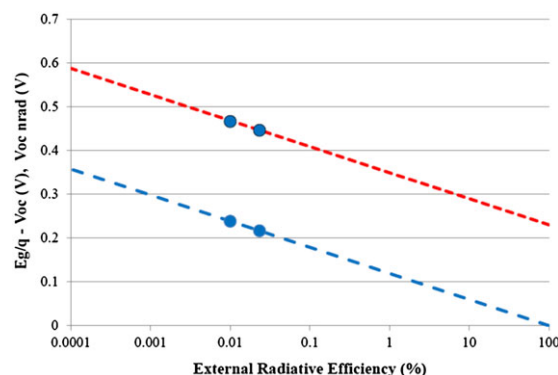


FIGURE 10 Open-circuit voltage drop compared with bandgap energy ($E_g/q - V_{oc}$) and nonradiative V_{oc} ($V_{oc, nrad}$) in perovskite solar cells as a function of external radiative efficiency (ERE) [Colour figure can be viewed at [wileyonlinelibrary.com](#)]

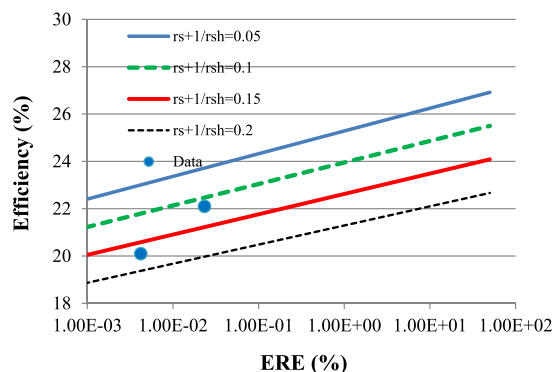


FIGURE 11 Calculated efficiency of perovskite solar cells as a function of external radiative efficiency (ERE) and $r_s + 1/r_{sh}$ [Colour figure can be viewed at wileyonlinelibrary.com]

5.4 | Efficiency potential of ferroelectric solar cells

The ferroelectric solar cells^{37–39} based on ferroelectric oxides have attracted significant attention owing to many unique advantages, such as the switchable photocurrent and photovoltage, and the high open-circuit voltages. However, the photocurrent densities under AM 1.5G solar illumination for most ferroelectric solar cells are very small, generally on the order of $\mu\text{A}/\text{cm}^2$ or nA/cm^2 , which greatly limit their PV performance with the conversion efficiency below 2%.³⁸ The small photocurrent densities are usually ascribed to the wide bandgap, poor light absorption coefficient, small charge carrier diffusion length, or low charge collection efficiency.³⁸ Recently, by bandgap tuning, new ferroelectric material such as $\text{Bi}_2\text{FeCrO}_6$, which exhibited both small bandgap (1.4–1.6 eV) and large photocurrent density ($20.6 \text{ mA}/\text{cm}^2$) with conversion efficiency of 8.1%, has been demonstrated.³⁹ However, device physics of the ferroelectric solar cells is still unknown.

Figure 12 shows V_{oc} drop compared with bandgap energy ($E_g/q - V_{oc}$) and nonradiative voltage loss ($V_{oc, \text{nrad}}$) in ferroelectric solar cell⁴⁰ as a function of ERE in comparison with those in GaAs, Si, and Perovskite solar cells. In the figure, ERE values estimated by using Equation 5 are plotted. In ferroelectric solar cells, 0.28 V was used as the $\Delta V_{oc, \text{rad}}$ value.⁴ As shown in Figure 12, ferroelectric solar cells have lower ERE from $10^{-6}\%$ to $3.8 \times 10^{-4}\%$ compared with 22.5%

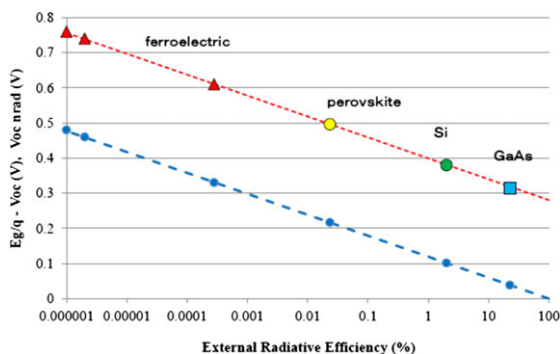


FIGURE 12 Open-circuit voltage (V_{oc}) drop compared with bandgap energy ($E_g/q - V_{oc}$) and nonradiative V_{oc} ($V_{oc, \text{nrad}}$) in ferroelectric solar cell as a function of external radiative efficiency (ERE) in comparison with those in GaAs, Si, and perovskite solar cells [Colour figure can be viewed at wileyonlinelibrary.com]

for GaAs⁴ and 8.71% for InGaP.⁸ Therefore, further improvements in efficiency by increasing ERE are necessary.

Figure 13 shows calculated efficiency of ferroelectric solar cells as a function of ERE and efficiency values for ferroelectric solar cells³⁹ in comparison with those of perovskite solar cells reported by KRICT^{22,35} and EPFL.³⁶ As shown in Figure 13, ferroelectric solar cells have lower external efficiency and higher resistance losses compared with perovskite solar cells. In summary, in the ferroelectric solar cells, efficiency of about 20% from present 8.1% efficiency³⁹ will be realized with $r_s + 1/r_{sh}$ of 0.2 by improvements in ERE into 1% from 10^{-6} to $3.8 \times 10^{-4}\%$ as shown in Figure 13.

6 | DISCUSSION ABOUT PATHWAY TOWARD REALIZING HIGHER EFFICIENCY SOLAR CELLS

As described above, further improvements in minority-carrier lifetime based on understanding defect behavior in addition to improvements in front surface, rear surface, and interface passivation and decrease in series resistance and increase in shunt resistance are thought to be very important to realize higher efficiency solar cells.

According to efficiency simulation for the crystalline Si solar cells by Swanson,⁴⁰ in the case of effective lifetime of 10 ms and 100 ms, efficiency potential of Si solar cells has shown an efficiency of 27.3% and 28%, respectively. It is suggested that the cell efficiency using practical and available silicon material is over 27%, providing that contacts with sufficiently low recombination can be realized.⁴⁰

Figure 14 shows calculated efficiency of crystalline Si solar cells as a function of effective minority-carrier life time in the case of $r_s + 1/r_{sh} = 0.05$ and in comparison with calculated results by Swanson⁴¹ and effective minority-carrier lifetime values τ_{eff} estimated from Yoshikawa et al, Green, and Yao et al^{1,4,5} by using Equations 5 and 13.

$$\text{ERE} = \text{InternalRadiativeEfficiency (IRE)} = \tau_{\text{eff}} / (\tau_{\text{rad}} + \tau_{\text{eff}}) \quad (14)$$

where τ_{rad} is radiative recombination lifetime and is given by Equation 1. As shown in Figure 14, higher efficiency of more than 27% by further improvement in minority-carrier lifetime is expected to be realized. Although the limiting efficiency for crystalline Si solar cells by

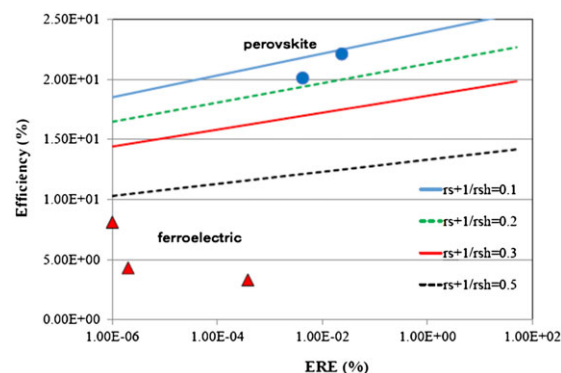


FIGURE 13 Calculated efficiency of ferroelectric solar cells as a function of external radiative efficiency (ERE) and $r_s + 1/r_{sh}$ in comparison with those of perovskite solar cells [Colour figure can be viewed at wileyonlinelibrary.com]

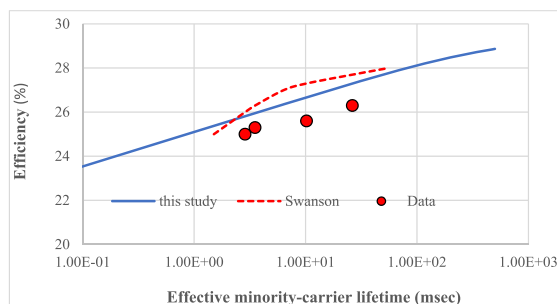


FIGURE 14 Calculated efficiency of crystalline Si solar cells as a function of effective minority-carrier life time in the case of $r_s + 1/r_{sh} = 0.05$ and in comparison with calculated results by Swanson and minority-carrier lifetime values estimated from references by using Equations 5 and 13. [Colour figure can be viewed at wileyonlinelibrary.com]

Auger recombination is 31.6%, calculated limiting efficiencies reported by Swanson⁴⁰ and Richter et al⁴¹ are 28.8% and 29.43%, respectively. Really, high bulk lifetime of around 100 ms has been obtained by the magnetic-field-applied Czochralski method and decreasing carbon concentration to less than 10^{14} cm^{-3} in Si.⁴² Therefore, improvement in Si crystalline quality and reduction in densities of defects such as dislocations, grain boundaries, and impurities that act as nonradiative recombination centers even in crystalline Si solar cells.

Because the effective lifetime is expressed by the following equation, front-surface, rear surface, and interface passivation are very effective for realizing higher efficiency.

$$1/\tau_{\text{eff}} = BN + 1/\tau_{\text{nonrad}} + 2S/d \quad (15)$$

where S is surface recombination velocity and d is layer thickness. As Swanson has discussed about importance of passivation and contacting the surfaces,⁴⁰ further improvements in front and rear surface passivation and passivated contacts are necessary. Significant effect with saturation current density J_0 has been shown. J_0 of 18 fA/cm^2 was estimated for Panasonic HIT solar cells with an efficiency of 24.7%, and 26.7% efficiency with J_0 of 2 fA/cm^2 and 27.3% efficiency with J_0 of less than 1 fA/cm^2 by further reduction in J_0 are expected to be realized.⁴⁰

Lattice mismatching also degrades solar cell properties by increase in interface recombination velocity due to misfit dislocations and threading dislocation generation. Lattice mismatch ($\Delta a/a_0$) dependence of interface recombination velocity (S_i) is semiempirically expressed by^{32,33}

$$S_i [\text{cm/s}] = 1.5 \times 10^8 \Delta a/a_0 \quad (16)$$

Therefore, lattice constant matching among active layers, buffer layers, and substrates is necessary to realize higher efficiency in the case of compound semiconductor solar cells.

As shown in Figures 6 and 13, resistance losses in the case of new materials solar cells such as CZTS(Se) and ferroelectric solar cells are much higher compared with GaAs and Si solar cells. To realize higher efficiency new materials solar cells, reduction in resistance losses by optimization of carrier concentration, increasing carrier mobility,

reduction in contact resistance, and increase of shunt resistance are necessary.

Photon recycling is thought to be very effective for improving V_{oc} , J_{sc} , and efficiency of solar cells. The highest 1-sun efficiency (Eff = 28.8%, $V_{oc} = 1.122 \text{ V}$, $J_{sc} = 29.68 \text{ mA/cm}^2$, FF = 86.5%) GaAs thin-film ($2.5 \mu\text{m}$ thick) single-junction solar cells have been demonstrated by the Alta Devices.²⁸ About 0.1 V higher V_{oc} compared with conventional GaAs solar cells has been attained due to photon recycling effect. Higher efficiency of more than 30% with GaAs thin-film solar cells is also expected to be realized by using strong internal and ERE.⁴³

7 | SUMMARY

Brief overviews of PV R&D projects in Japan are presented. Recently, world-record and second highest efficiencies of various types of solar cells have been demonstrated under the NEDO Project: 44.4% (under concentration) and 37.9% (under 1-sun) InGaP/GaAs/InGaAs inverted metamorphic 3-junction solar cells by Sharp, 26.7% single crystalline Si HBC solar cell by Kaneka, 22.3% CIGS solar cell by Solar Frontier, a-Si/ $\mu\text{c-Si}/\mu\text{c-Si}$ thin-film triple-junction solar cell with stabilized efficiency of 14.0% by AIST, 11.9% dye-sensitized solar cell by Sharp, and 11.2% organic solar cell by Toshiba.

Efficiency potential of high-efficiency solar cells such as crystalline Si, GaAs, III-V compound 3-junction and 5-junction, CIGSe, CdTe cells, and next-generation solar cells such as CZTS(Se), MQW and QD, Perovskite, and ferroelectric solar cells is discussed based on ERE, V_{oc} loss, and FF loss.

In summary,

1. Crystalline Si solar cells have potential efficiency of 28.8% with normalized series resistance and shunt resistance $r_s + 1/r_{sh}$ of 0.05 by improvements in ERE from around 1% to 30%.
2. GaAs have potential efficiency of 30.0% with $r_s + 1/r_{sh}$ of 0.025 by improvements in ERE from 22.5% to 40%.
3. III-V 3-junction and 5-junction cells have potential efficiencies of 40% and 43% with $r_s + 1/r_{sh}$ of 0.05 by improvements in ERE from 0.05% to 1% and from 0.005% to 1%, respectively.
4. CIGSe and CdTe cells have potential efficiencies of 26.5% and 26.4% with $r_s + 1/r_{sh}$ of 0.05 by improvements in ERE from around 0.5% to 10% and from around 0.1% to 5%, respectively.
5. CZTS(Se) and CIGS solar cells have efficiency potential of more than 20% and 22%, respectively, by improvement in ERE from around about 0.001% to 1%.
6. MQW and QD cells have efficiency potential of 24.8% and 25.8% by improvements in ERE from around 0.1% to 1% and 10%, respectively.
7. Perovskite cells have potential efficiencies of 24.0% and 24.9% by improvements in ERE from about 0.02% to 1% and 10%, respectively.
8. Although the ferroelectric solar cells have shown unique properties, 8.1% efficiency has been demonstrated. Efficiency of about 20% from present 8.1% efficiency will be realized with $r_s + 1/r_{sh}$ of 0.2 by improvements in ERE into 1% from 10^{-6} to $3.8 \times 10^{-4}\%$.

Pathway toward realizing higher efficiency solar cells is also discussed. Further improvements in minority-carrier lifetime based on understanding defect behavior in addition to improvements in front surface, rear surface, and interface passivation and decrease in series resistance and increase in shunt resistance are suggested to realize higher efficiency solar cells.

ACKNOWLEDGEMENTS

The author thanks members in the NEDO, METI, and JST and Prof Y Ohshita, Prof A Yamamoto, and Dr Y Hayashi, Toyota Tech Inst; Dr H Sai, Dr Tampo, and Dr Shibata, AIST; Dr H Sugimoto and Dr H Hiroi, Solar Frontier; Y Kanemitsu, Kyoto Univ; and H Akiyama, Univ Tokyo, for their cooperation and providing fruitful information.

ORCID

Masafumi Yamaguchi  <http://orcid.org/0000-0002-2825-7217>

Kan-Hua Lee  <http://orcid.org/0000-0001-8560-1515>

Kenji Araki  <http://orcid.org/0000-0002-3216-948X>

REFERENCES

- Yoshikawa K, Kawasaki H, Yoshida W, et al. Silicon heterojunction solar cell with interdigitated back contacts for a photoconversion efficiency over 26%. *Nat Energ*. 2017;2:17032.
- Ahrenkiel RK. *Semiconductors and Semimetals*. Vol. 39, eds. Ahrenkiel RK and Lundstrom MS. (Academic Press, Boston) p.58.
- Rau U. Reciprocity relation between photovoltaic quantum efficiency and electroluminescent emission of solar cells. *Phys Rev B*. 2007;76:085303.
- Green MA. Radiative efficiency of state-of-the-art photovoltaic cells. *Prog Photovoltaics*. 2012;20:472.
- Yao J, Kirchartz T, Vezie MS, et al. Quantifying losses in open-circuit voltage in solution-processable solar cells. *Phys Rev Applied*. 2015;4:014020.
- Green MA, Emery K, Hishikawa Y, Warta W. Solar cell efficiency tables (version 36). *Prog Photovoltaics*. 2010;18:346.
- Green MA, Emery K, Hishikawa Y, Warta W. Solar cell efficiency tables (version 37). *Prog Photovoltaics*. 2011;19:84.
- Geisz JF, Steiner MA, Garcia I, Kurtz SR, Friedman DJ. Enhanced external radiative efficiency for 20.8% efficient single-junction GaInP solar cells. *Appl Phys Lett*. 2013;103:041118.
- Kamada R, Yagioka T, Adachi S, et al. New world record Cu(In, Ga)(Se, S)₂ thin film solar cell efficiency beyond 22%. Proceedings of the 43rd IEEE Photovoltaic Specialists Conference. 2016 p.1287.
- Green MA, Emery K, Hishikawa Y, et al. Solar cell efficiency tables (version 49). *Prog Photovoltaics*. 2017;25:3.
- Ishizuka S, Yamada A, Fons PJ, Shibata H, Niki S. Structural tuning of wide-gap chalcopyrite CuGaSe₂ thin films and highly efficient solar cells: Differences from narrow-gap Cu(In,Ga)Se₂. *Prog Photovoltaics*. 2014;22:821.
- Hiroi H, Iwata Y, Sugimoto H, Yamada A. Over 16% efficiency of Se-free Cu(In,Ga)S₂ solar cell. *E-MRS 2017 Spring Meeting*. 2017; E.VII.1.
- Nayak PK, Cahen D. Updated assessment of possibilities and limits for solar cells. *Adv Mater*. 2014;26:1622.
- Wang W, Winkler MT, Gunawan O, et al. Device characteristics of CZTSSe thin-film solar cells with 12.6% efficiency. *Adv Energ Mater*. 2014;4:1301485.
- Sugimoto H, Liao C, Hiroi H, Sakai N, Kato T. Lifetime improvement for high efficiency Cu₂ZnSnS₄ submodules. Proceedings of the 39th IEEE Photovoltaic Specialists Conference. 2013 p.3208. <http://doi.org/10.1109/PVSC.2013.6745135>
- Wang Y, Wen Y, Sodabanlu H, Watanabe K, Sugiyam M, Nakano Y. A superlattice solar cell with enhanced short-circuit current and minimized drop in open-circuit voltage. *IEEE J Photovoltaics*. 2012;2:387.
- Okada Y, Ekins-Daukes NJ, Kita T. Intermediate band solar cells: Recent progress and future directions. *Appl Phys Rev*. 2015;2:2.
- Green MA. *Solar Cells*. Kensington: UNSW; 1998.
- Taguchi M, Yano A, Tohoda S, et al. 24.7% Record efficiency HIT solar cell on thin silicon wafer. *IEEE J Photovoltaics*. 2014;4:96.
- Masuko K, Shigematsu M, Hashiguchi T, et al. Achievement of More Than 25% Conversion Efficiency With Crystalline Silicon Heterojunction Solar Cell. *IEEE J Photovoltaics*. 2014;4:1433.
- Zhao J, Wang A, Green MA, Ferrazza F. 19.8% efficient "honeycomb" textured multicrystalline and 24.4% monocrystalline silicon solar cells. *Appl Phys Lett*. 1998;73:1991.
- Green MA, Emery K, Hishikawa Y, Warta W, Dunlop ED. Solar cell efficiency tables (version 48). *Prog Photovoltaics*. 2016;24:905.
- Katagiri H, Jimbo K, Yamada S, et al. Enhanced Conversion Efficiencies of Cu₂ZnSnS₄-Based Thin Film Solar Cells by Using Preferential Etching Technique. *Appl Phys Express*. 2008;1:041201.
- Hiroi H, Iwata Y, Adachi S, Sakai N, Sugimoto H. New World-Record Efficiency for Pure-Sulfide Cu(In,Ga)S₂ Thin-Film Solar Cell With Cd-Free Buffer Layer via KCN-Free Process. *IEEE J Photovoltaics*. 2016;6:760.
- Hiroi H, Sakai N, Iwata Y, Kato T, Sugimoto H. Impact of buffer layer on kesterite solar cells. Proceedings of the 42nd IEEE Photovoltaic Specialists Conference. 2015 p. 3625.
- Barnham KWJ, Duggan G. A new approach to high-efficiency multi-band-gap solar cells. *J Appl Phys*. 1990;67:3490.
- Luque A, Marti A. Increasing the efficiency of ideal solar cells by photon induced transitions at intermediate levels. *Phys Rev Lett*. 1997;78:5014.
- Kayes BM, Nie H, Twist R, et al. 27.6% Conversion efficiency, a new record for single-junction solar cells under 1 sun illumination. Proceedings of the 37th IEEE Photovoltaic Specialists Conference. 2011 p. 4.26.
- Blokhin SA, Sakharov AV, Nadtochy AM, et al. AlGaAs/GaAs photovoltaic cells with an array of InGaAs QDs. *Semiconductors*. 2009;43:514.
- Okada Y, Ohshima R, Takata A. Characteristics of InAs/GaNAs strain-compensated quantum dot solar cell. *J Appl Phys*. 2009;106:024306.
- Bailey CG, Forbes DV, Raffaele RP, Hubbard SM. Near 1 V open circuit voltage InAs/GaAs quantum dot solar cells. *Appl Phys Lett*. 2011;98:163105.
- Neuse CJ. III-V alloys for optoelectronic applications. *J Electron Mater*. 1977;6:253.
- Yamaguchi M. Fundamentals and R&D status of III-V compound solar cells and materials. *Phys Status Solidi C*. 2015;12:489.
- Kojima A, Toshima K, Shirai Y, Miyasaka T. Organometal Halide Perovskites as Visible-Light Sensitizers for Photovoltaic Cells. *J Am Chem Soc*. 2009;131:6050.
- Yang WS, Noh JH, Jeon NJ, et al. High-performance photovoltaic perovskite layers fabricated through intramolecular exchange. *Science*. 2015;348:L234.
- Song Z, Abate A, Watthage SC, et al. In-situ observation of moisture-induced degradation of perovskite solar cells using laser-beam induced current. 43rd IEEE Photovoltaic Specialists Conference. Portland, USA, June 5-10 2016.
- Spanier JE, Fridkin VM, Rappe AM, et al. Power conversion efficiency exceeding the Shockley-Queisser limit in a ferroelectric insulator. *Nat Photon*. 2016;10:611.
- Chen B, Shi J, Zheng X, Zhou Y, Zhuc K, Shashank P. Ferroelectric solar cells based on inorganic-organic hybrid perovskites. *J Mater Chem A*. 2015;3:7699.
- Nechachel R, Harnagea C, Li S, et al. Bandgap tuning of multiferroic oxide solar cells. *Nat Photon*. 2015;9:61.

40. Swanson RM. Approaching the 29% limit efficiency of silicon solar cells, Photovoltaic Specialists Conference, 2005. Conference Record of the Thirty-first IEEE.
41. Richter A, Hermle M, Glunz SW. Reassessment of the limiting efficiency for crystalline silicon solar cells. *IEEE J Photovoltaics*. 2013;3:31184.
42. Higasa M, Nagai Y, Nakagawa S, Kashima K. Effect of low carbon concentration on bulk carrier lifetime in MCZ silicon crystal. Abstract of the 75th annual meeting of the Japan Society of Applied Physics. 2014:20a-A20-3.
43. Miller OW, Yablonovitch E, Kurtz SR. Strong internal and external luminescence as solar cells approach the Shockley-Queisser limit. *IEEE J Photovoltaics*. 2012;2:303.

How to cite this article: Yamaguchi M, Lee K-H, Araki K, Kojima N, Yamada H, Katsumata Y. Analysis for efficiency potential of high-efficiency and next-generation solar cells. *Prog Photovolt Res Appl*. 2018;26:543–552. <https://doi.org/10.1002/pip.2955>